

# **ON THE DEFLECTION OF S32003 STAINLESS STEEL BEAMS**

A Thesis  
Presented to  
The Academic Faculty

by

Eman Said

In Partial Fulfillment  
of the Requirements for the Degree  
Master of Science in the  
School of Civil and Environmental Engineering

Georgia Institute of Technology  
May 2016

**COPYRIGHT © 2015 BY EMAN SAID**

# **ON THE DEFLECTION OF S32003 STAINLESS STEEL BEAMS**

Approved by:

Dr. Abdul-Hamid Zureick, Advisor  
School of Civil and Environmental Engineering  
*Georgia Institute of Technology*

Dr. Rafi L. Muhanna  
School of Civil and Environmental Engineering  
*Georgia Institute of Technology*

Dr. David W. Scott  
School of Civil and Environmental Engineering  
*Georgia Institute of Technology*

Date Approved: January 13, 2016

## **ACKNOWLEDGEMENTS**

I would like to express my sincere gratitude to my advisor, Dr. Abdul-Hamid Zureick. Without his guidance, patience, and support this work would not have been possible. He taught me about the nature of research and encouraged me to strive for excellence in the work I produce. His availability made it possible for me to ask questions, learn, and finish my thesis in a timely manner.

I would also like to thank my other thesis committee members: Dr. Rafi Muhanna and Dr. David Scott, for reviewing my work and providing insightful comments. Additionally, I offer my appreciation to Dr. Scott for teaching me how to use the equipment in the lab, which was a critical part of my research.

I would like to thank my friend, Dr. Haitham Eletrabi for his constant support and encouragement, and for his faith in my capacity. His humor, and optimism helped me to keep a positive attitude throughout the process of writing my thesis. I also express sincere appreciation to my family: my parents, Nadera and Abdul-Hussain, and my sister, Noura, for supporting me throughout this thesis and throughout my life in general. I also express my gratitude to my brother, Hamid for his helpful discussions. They have shaped who I am today and I would not have been pursuing my master's degree if it was not for them. I am grateful to my aunt, Victoria, who provided me with a healthy environment to work and focus, and to all my friends who kept me in their prayers.

## TABLE OF CONTENTS

ACKNOWLEDGEMENTS .....	iii
LIST OF TABLES .....	v
LIST OF FIGURES .....	vi
LIST OF SYMBOLS .....	viii
SUMMARY .....	x
CHAPTER 1: INTRODUCTION .....	1
1.1 Motivation .....	1
1.2 Objective and Scope .....	1
1.3 Thesis Outline .....	1
CHAPTER 2: STAINLESS STEEL MATERIALS .....	3
2.1 The Development of Stainless Steel .....	3
2.2 Chemical Composition of Stainless Steel .....	4
2.3 Corrosion Properties of Stainless Steels .....	5
2.4 Welding Process of Stainless Steel .....	8
2.5 Stress-Strain Relationship of Stainless Steel .....	9
CHAPTER 3: DEFLECTION OF FULL-SECTION STAINLESS STEEL MEMBERS .....	11
CHAPTER 4: EXPERIMENTS .....	17
4.1 Test Specimen Material .....	17
4.2 Test Specimens .....	20
4.3 Testing Procedure and Results .....	22
4.4 Analyses of Results .....	26
4.5 Deflection Calculation Method .....	28
CHAPTER 5: CONCLUSIONS AND RECOMMENDATIONS .....	32
REFERENCES .....	33

## LIST OF TABLES

	Page
Table 2.1. Chemical composition of duplex and austenitic stainless steel .....	5
Table 2.2. Pitting resistance equivalent number for duplex and austenitic stainless steel types .....	7
Table 2.3. Mechanical properties of austenitic and duplex stainless steels .....	10
Table 3.1. Reported dimensions of two stainless steel beams (S30400) used for flexural test from Rasmussen and Hancock (1993).....	12
Table 3.2. Dimension of SHS 80x80 stainless steel beam (S30400) used for three-point flexural test from Mirambell and Real (2000) .....	13
Table 3.3. Dimension of S32012 beams used for three-point flexure test from Theofanous and Gardner (2010) .....	14
Table 3.4. Dimensions of S32101 beams used for three-point flexure test from Saliba and Gardner (2012).....	16
Table 4.1. Results from tensile testing on welded S32003 samples .....	20
Table 4.2. Test specimen dimensions .....	22

# LIST OF FIGURES

	Page
Figure 2.1. Duplex stainless steel Celtic Gateway footbridge in Holyhead, UK.....	4
Figure 2.2. Duplex stainless steel roof at Hamad International Airport, Qatar .....	4
Figure 2.3. CPT and CCT for unwelded austenitic and duplex stainless steels.....	8
Figure 2.4. Stress-strain curves for different types of carbon and stainless steels.....	9
Figure 3.1. Load-deflection curve for SHS80x80 beam (S30403) from Mirambell and Real (2000).....	13
Figure 3.2. Moment vs. rotation curves for SHS and RHS S32101 beams from Theofanous and Gardner (2010) .....	15
Figure 3.3. Moment vs. rotation curves from 3-point bending test for four I-section S32101 beams from Saliba and Gardner (2012).....	16
Figure 4.1. Critical Pitting Temperature of austenitic and duplex stainless steels .....	18
Figure 4.2. Critical Crevice Temperature of austenitic and duplex stainless steels .....	19
Figure 4.3. Results of charpy impact test on S32003 welded plate (ATI Allegheny Ludlum 2010).....	19
Figure 4.4. Three-point flexural test set up.....	23
Figure 4.5. Load-deflection curves of all specimens .....	23
Figure 4.6. Load-deflection curves of specimens with 4in span length.....	24
Figure 4.7. Load-deflection curves of specimens with 6in span length.....	24
Figure 4.8. Load-deflection curves of specimens with 9in span length.....	25
Figure 4.9. Load-deflection curves of specimens with 12in span length.....	25
Figure 4.10. Cross-section strain and stress distribution of S32003 stainless steel.....	28
Figure 4.11. Experimental and theoretical results of load-deflection curves for specimens with 4in span length .....	30

Figure 4.12. Experimental and theoretical results of load-deflection curves for specimens with 6in span length .....	30
Figure 4.13. Experimental and theoretical results of load-deflection curves for specimens with 9in span length .....	31
Figure 4.14. Experimental and theoretical results of load-deflection curves for specimens with 12in span length .....	31

## LIST OF SYMBOLS

$A$	Cross-sectional Area
$a$	Weld Throat
$b$	Width
$d$	Depth
$E$	Flexural Modulus
$E_{as}$	Average Secant Modulus
$E_o$	Initial Modulus
$E_{ts}$	Tensile Secant Modulus
$E_{cs}$	Compression Secant Modulus
$E_s$	Secant Modulus
$e$	Ratio of the deflection due to shear to that due to flexure
$G$	Shear Modulus
$h$	Height of Web
$I$	Moment of Inertia
$L$	Span Length
$M$	Moment
$n$	Material Constant
$P$	Load
$t$	Thickness
$t_f$	Thickness of Flange
$t_w$	Thickness of Web

$y_c$	Location of the compression/tension force with respect to the neutral axis
$\alpha$	Shear Coefficient
$\delta$	Deflection
$\varepsilon$	Strain
$\varepsilon_{max}$	Maximum Strain
$\theta$	Rotation
$\sigma$	Stress
$\sigma_{max}$	Maximum Stress
$\nu$	Poisson's Ratio

## SUMMARY

UNS S32003 duplex stainless steel is an attractive candidate for use in civil engineering infrastructure applications due to its corrosion resistance properties, high strength, and reasonable cost. Because of the limited technical information related to material characterization, behavior, and design of this particular stainless steel grade, UNS S32003 duplex stainless steel is not currently covered in any national or international civil engineering design guideline and standard. All standards require that both strength and serviceability limit states be addressed. Deflection calculations of stainless steel structures require that the load-deflection behavior of stainless steel be understood.

Presented in this work are the results of twelve flexural tests conducted on small-scale coupons to establish the load-deflection behavior of UNS S32003 (ATI 2003®) hot-rolled duplex stainless steel flat plates. All specimens were tested as simply supported beams loaded at the midspan. Test specimens had nominal width and thickness of 1 in. and 0.25 in., respectively. Four different span lengths of 4 in., 6 in., 9 in., and 12 in. were investigated. Analyses of the results showed that the non-linear deflection behavior can be estimated reasonably well by adopting the conventional deflection equation pertaining to an assumed linear elastic material, but after replacing the modulus of elasticity with a secant modulus corresponding to the maximum tension strain resulting from the applied load.

# **CHAPTER 1**

## **INTRODUCTION**

### **1.1 Motivation**

In recent years, S32003 duplex stainless steel has attracted attention as a viable structural material because of its high strength, corrosion resistance, and cost. Understanding the load-deflection behavior of S32003 stainless steel is important for inclusion in design guidelines and standards. As for most stainless steel grades, the deflection behavior of S32003 beams subjected to transverse loads is non-linear and the use of the traditional deflection equation for calculating the deflection of linearly elastic material yields an underestimate of the computed deflection values.

### **1.2 Objective and Scope**

The objective of this work is to examine the load-deflection behavior of stainless steel beams. This objective is achieved by conducting a three-point flexural test on small-scale specimens and comparing the results with those obtained from computing the deflection using the conventional deflection equation of linearly elastic materials, but after replacing the modulus of elasticity with a secant modulus corresponding to the maximum tension strain resulting from the applied load.

### **1.3 Thesis Outline**

The introduction is presented here, in Chapter 1. Chapter 2 provides background information on stainless steel materials, which includes the chemical composition, corrosion properties, relevant mechanical properties and welding procedures for

commonly available stainless steel materials. In Chapter 3, brief reviews are presented on works addressing the deflection of full-section stainless steel members. Chapter 4 provides a brief introduction to S32003 duplex stainless steel, the material used for experiments in this thesis. Furthermore, Chapter 4 covers the experimental investigation and the major findings resulted from this research program. Finally, Chapter 5 presents the conclusions and recommendations for further research.

## **CHAPTER 2**

### **STAINLESS STEEL MATERIALS**

#### **2.1 The Development of Stainless Steel**

Developed in the twentieth century, stainless steel is a ferrous alloy that has a chromium content ranging from 11% to 30% (Lula 1986). There are five basic groups of stainless steel, which are classified according to their metallurgical structure: austenitic, ferritic, martensitic, duplex, and precipitation-hardening groups. Austenitic stainless steels are known to provide a good combination of corrosion resistance, forming, and fabrication properties. On the other hand, duplex stainless steels have very good resistance to stress corrosion cracking and high strength and wear resistance (SCI 2006).

Duplex Stainless steels are ferritic/austenitic alloys with 30%-70% ferrite. Compared with austenitic stainless steels, duplex stainless steels have less nickel content. In the 1950s and late 1960s, shortages in nickel increased the price of austenitic stainless steels, which advanced the development and encouraged the use of duplex stainless steels (Gunn 1997). Different grades of duplex stainless steels have been used in civil engineering construction all over the world. Examples include, among others, the 2006 stainless steel Celtic Gateway footbridge in Holyhead, UK (Figure 2.1) and the world's largest stainless steel roof in the new Hamad International Airport in Qatar, which was constructed in 2014 (Figure 2.2).



Figure 2.1. Duplex stainless steel Celtic Gateway footbridge in Holyhead, UK (Courtesy of Ren Whithnell)



Figure 2.2. Duplex stainless steel roof at Hamad International Airport, Qatar (Courtesy of Hamad International Airport)

## 2.2 Chemical Composition of Stainless Steel

Table 2.1 shows the chemical composition of common austenitic and duplex stainless steel types (ASTM A240/A240M 2015). The steel grades are designated in the table according to the American Iron and Steel Institute (AISI), the Unified Numbering System (UNS), and the European Norm (EN). Commonly available lean duplex grades ( $\text{Cr} > 17\%$  and  $\text{Mo} < 1\%$ ) are also tabulated.

Table 2.1. Chemical composition for common types of duplex and austenitic stainless steel

<b>Stainless Steel Type</b>	<b>AISI Grade</b>	<b>UNS No.</b>	<b>EN No.</b>	<b>Cr</b>	<b>Ni</b>	<b>Mo</b>	<b>N</b>	<b>Cu</b>	<b>Mn</b>
<b>Austenitic</b>	304L	S30403	1.4307	17.5-19.5	8.0-12	-	0.1	-	2
<b>Austenitic</b>	316L	S31603	1.4404	16.0-18.0	10-14	2.0-3.0	0.1	-	2
<b>Duplex</b>	2003	S32003		19.5-22.5	3.0-4.0	1.5-2.0	0.14-0.2	-	2
<b>Duplex</b>	2205	S32205	1.4462	22.0-23.0	4.5-6.5	3.0-3.5	0.14-0.2	-	2
<b>Lean Duplex</b>	2001	S32001	1.4482	19.5-21.5	1.0-3.0	0.6	0.05-0.17	1	4.0-6.0
<b>Lean Duplex</b>	2101	S32101	1.4162	21.0-22.0	1.35-1.7	0.1-0.8	0.2-0.25	0.1-0.8	4.0-6.0
<b>Lean Duplex</b>	2202	S32202	1.4062	21.5-24.0	1.0-2.8	0.45	0.18-0.26	-	2
<b>Lean Duplex</b>	2304	S32304	1.4362	21.5-24.5	3.0-5.5	0.05-0.6	0.05-0.2	0.05-0.6	2.5

\*All stainless steel types have 0% tungsten (W)

## 2.3 Corrosion Properties of Stainless Steels

Stainless Steel is a term covering a large group of alloys that are known for their corrosion resistance (Parr and Hanson 1966). Corrosion is the deterioration of a material, which results from a chemical or electrochemical reaction with its environment (ASTM G193-12 2012). Commonly known forms of corrosion in stainless steel are: general, pitting, crevice, galvanic, intergranular, and stress corrosion cracking, defined as follows, according to ASTM G193-12 (2012) and ASTM G157-13 (2013):

- General corrosion: corrosion that is distributed more-or-less uniformly over the surface of a material.
- Pitting corrosion: Localized corrosion of a metal surface confined to a small area and takes the form of cavities called pits.
- Crevice corrosion: Localized corrosion of a metal or alloy surface at, or immediately adjacent to, an area that is shielded from full exposure to the environment because of proximity of the metal or alloy to the surface of another material or an adjacent surface of the same metal or alloy.

- Galvanic corrosion: accelerated corrosion of a metal because of an electrical contact with a more noble metal or nonmetallic conductor in a corrosive electrolyte.
- Intergranular corrosion: preferential corrosion at or adjacent to the grain boundaries of a metal or alloy.
- Stress corrosion cracking: cracking of a material produced by the combined action of corrosion and sustained tensile stress (residual or applied).

Compared to other types of steel, stainless steel has a better resistance to general corrosion due to its high chromium content that facilitates the development of a passive oxide film that resists general corrosion. Regarding pitting corrosion, various equations have been developed to present a single pitting resistance equivalent number (PREN) for ranking and comparing different grades of stainless steel materials. NACE/ASTM G193-12 (2012) references the following PREN equation based on weight content of chromium (Cr), molybdenum (Mo), nitrogen (N), and tungsten (W):

$$\text{PREN} = \% \text{ wt Cr} + 3.3(\% \text{ wt Mo} + 0.5(\% \text{ wt W})) + 16(\% \text{ wt N}) \quad (2.1)$$

Table 2.2 shows the calculated pitting resistance equivalent number (PREN) of different grades of austenitic and duplex stainless steels, using Eq. 2.1.

Table 2.2. Pitting resistance equivalent number (PREN) for duplex and austenitic stainless steel types

<b>Stainless Steel Type</b>	<b>AISI Grade</b>	<b>UNS No.</b>	<b>EN No.</b>	<b>PREN</b>
<b>Austenitic</b>	304L	S30403	1.4307	21-23
<b>Austenitic</b>	316L	S31603	1.4404	26-31
<b>Duplex</b>	2003	S32003	-	29-35
<b>Duplex</b>	2205	S32205	1.4462	36-41
<b>Lean Duplex</b>	2001	S32001	14482	23-29
<b>Lean Duplex</b>	2101	S32101	1.4162	27-32
<b>Lean Duplex</b>	2202	S32202	1.4062	28-33
<b>Lean Duplex</b>	2304	S32304	1.4362	23-32

Of greater importance are the determination of the critical pitting temperature (CPT) and critical crevice temperature (CCT), which help determine when pitting and crevice corrosion occur. Critical pitting temperature is the minimum temperature (°C) that causes pitting attack, at least, 0.025-mm (0.001-in.) deep on the bold surface of a stainless steel specimen as defined in ASTM G48 (2011). The critical crevice temperature is the minimum temperature (°C) that causes crevice attack, at least, 0.025-mm (0.001-in.) deep on the bold surface of a stainless steel specimen beneath the crevice washer as stipulated in ASTM G48 (2011). Figure 2.3 shows the CPT and CCT values for austenitic and duplex stainless steels in the solution annealed condition, evaluated in 6% ferric chloride per ASTM G48 (IMO, 2014).

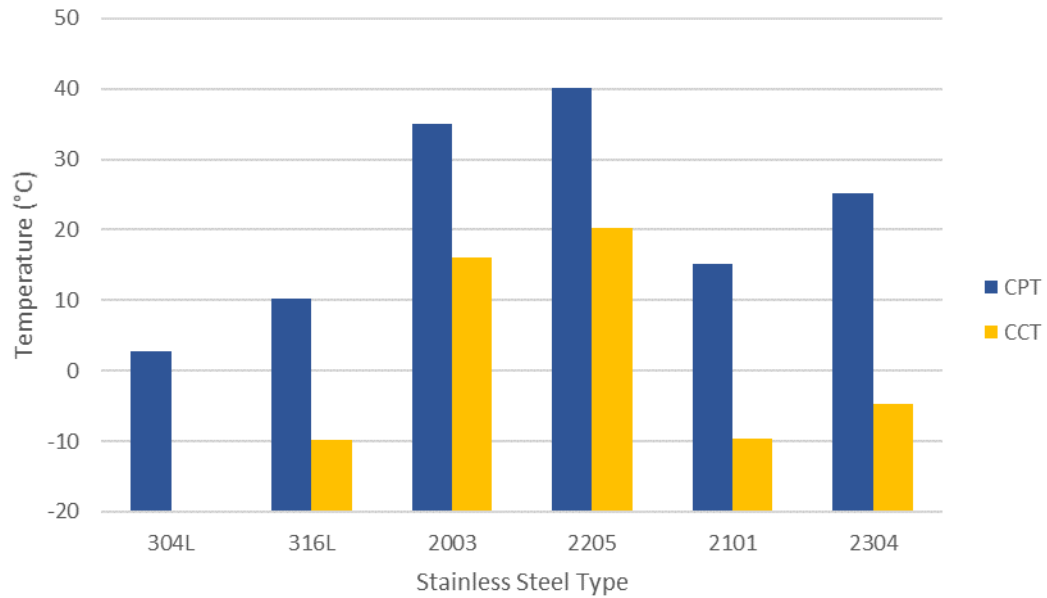


Figure 2.3. CPT and CCT for unwelded austenitic and duplex stainless steels (IMOA, 2014)

## 2.4 Welding Process of Stainless Steel

The welding process for stainless steels should ideally provide a sound joint that has qualities equal to or better than those of the base material (AISI, 1988). There are many types of welding processes for stainless steel. The more established processes are defined in the American Welding Society (AWS) D1.6 Structural Welding Code-Stainless Steel. These welding processes include the shielded metal arc welding (SMAW), gas tungsten arc welding (GTAW), gas metal arc welding (GMAW), submerged arc welding (SAW), flux cored arc welding (FCAW), and plasma arc welding (PAW). The selection of the welding process and procedure depends on the thickness of the material, type of joint, fabrication economics, and other design factors (Gunn, 1997).

## 2.5 Stress-Strain Relationship of Stainless Steel

The full-range tensile stress-strain curves of stainless steel material is generally different from those of carbon steels. For examples, the stress-strain curve of stainless steel materials does not have a well-defined yield stress point as is the case for low-carbon steel materials. The yield stress of stainless steel materials is often determined from the 0.2% offset strain method outlined in ASTM A370, as is the case for high-strength steel materials. In addition, unlike the stress-strain curve of carbon steel, which can be reasonably represented by a linear function, the stress-strain curve for stainless steel material exhibits nonlinear behavior from the beginning of the curve. The stress-strain curves for various stainless steel and carbon steel materials are presented in Figure 2.4 (Rasmussen 2002; Tavares et al. 2012; Wright 2012). Table 2.3 shows the minimum values of tensile and yield strength of different austenitic and duplex stainless steels according to ASTM A240/A240M (2015) specification for stainless steel plates and sheets and general applications.

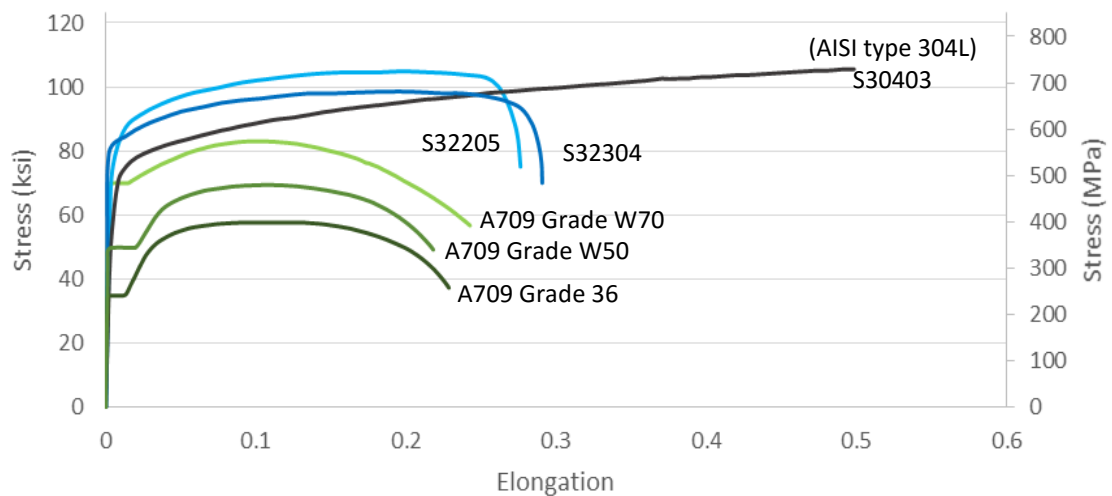


Figure 2.4. Stress-strain curves for different types of carbon and stainless steels

Table 2.4. Mechanical properties of different types of austenitic and duplex stainless steels

Stainless Steel Type	AISI Grade	UNS No.	EN No.	Tensile Strength, min		Yield Strength, min		Elongation in 2in. or 50mm, min	Notes
				ksi	MPa	ksi	MPa	%	
<b>Austenitic</b>	304L	S30403	1.4307	70	485	25	170	40	
<b>Austenitic</b>	316L	S31603	1.4404	70	485	25	170	40	
<b>Duplex</b>	2003	S32003	-	100	690	70	485	25	$t \leq 0.187\text{in}$ (5mm)
				95	655	65	450	25	$t \geq 0.187\text{in}$ (5mm)
<b>Duplex</b>	2205	S32205	1.4462	95	655	65	450	25	
<b>Lean Duplex</b>	2001	S32001	14482	90	620	65	450	25	
<b>Lean Duplex</b>	2101	S32101	1.4162	101	700	77	530	30	$t \leq 0.187\text{in}$ (5mm)
				94	650	65	450	30	$t \geq 0.187\text{in}$ (5mm)
<b>Lean Duplex</b>	2202	S32202	1.4062	94	650	65	450	30	
<b>Lean Duplex</b>	2304	S32304	1.4362	87	600	58	400	25	

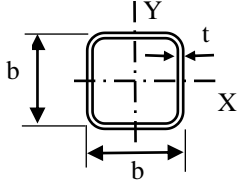
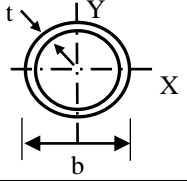
## **CHAPTER 3**

### **DEFLECTION OF FULL-SECTION STAINLESS STEEL MEMBERS**

Research focusing on the deflection of full-section stainless steel members subjected to transverse loading has been very limited in the literature. Of interest to this work are the studies by Rasmussen and Hancock (1993), Mirambell and Real (2000), Theofanous and Gardner (2010), and Saliba and Gardner (2012). Brief reviews of these studies are provided below.

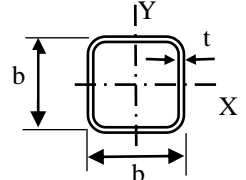
**Rasmussen and Hancock (1993):** In this study, two flexural tests were conducted on S30400 austenitic cold-formed stainless steel square hollow sections (SHS) and circular hollow sections (CHS) (Table 3.1). These tests were loaded symmetrically at two locations at distances equal to one-fourth of the span length from the supports. The load and the vertical deflections at mid-span and at the load locations were all recorded. The moment-curvature curves for these tests showed that the proportional limit of the SHS beam corresponded to approximately 40% of the yielding point of the material. Furthermore, the moment-curvature of the CHS beam exhibited a higher proportional limit than that of the SHS beam. It was also demonstrated that the use of an average secant modulus, proposed by Johnson and Winter (1966), in the deflection formula of a linear elastic beam yields excellent approximation of the experimentally measured deflection data.

Table 3.1. Reported dimensions of two stainless steel beams (S30400) used for flexural test from Rasmussen and Hancock (1993)

Tested Beam	Span length (in)	b (in)	t (in)	I (in <sup>4</sup> )	Cross-section Shape
S1B1	39.37	3.15	0.12	34370.1	
C1B1	39.37	4.02	0.11	42913.4	

**Mirambell and Real (2000):** In this work, the authors presented results of flexural tests conducted on six simply supported S30400 stainless steel beams subjected to a concentrated load at mid-span, and six S30400 stainless steel continuous beams subjected to concentrated loads at mid-span. Test beam cross sections had square hollow sections, rectangular hollow sections, and I-sections. The dimensions of one of the tested beams (SHS 80x80) is shown in Table 3.2. All load-deflection curves showed non-linear behavior as shown in Figure 3.1 for the SHS 80x80 beam. The authors compared various methods of calculating deflection values and concluded that the deflection calculation methods proposed by Rasmussen and Hancock (1993) and by the Eurocode 3 provide good approximations for the deflection values obtained experimentally. They also showed that when the deflection calculation is performed by considering the variation of the material modulus of elasticity along the length of the beam, the computed deflection values correlate well with those obtained experimentally.

Table 3.2. Dimension of SHS 80x80 stainless steel beam (S30400) used for three-point flexural test from Mirambell and Real (2000)

Tested Beam	Total Length (in)	Span length (in)	b (in)	t (in)	Cross-section Shape
SHS 80x80	78.74	70.87	3.15	0.12	

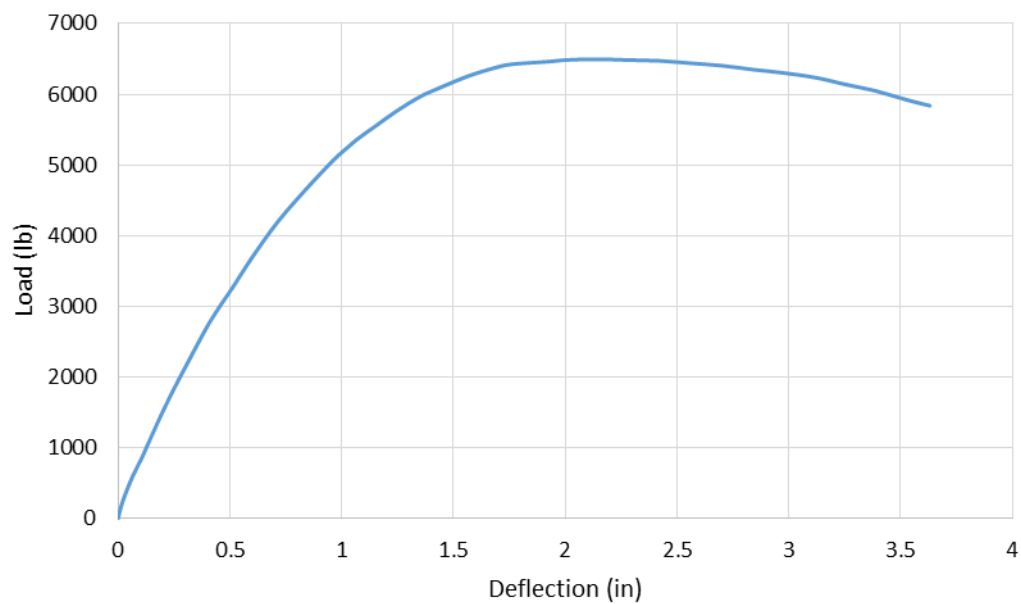
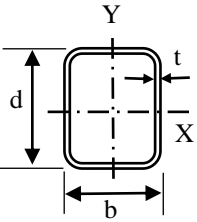


Figure 3.1. Load-deflection curve for SHS80x80 beam (S30403) from Mirambell and Real (2000)

**Theofanous and Gardner (2010):** In this experimental program, eight three-point bending tests were conducted on S32101 lean duplex stainless steel tubular beams. Six square hollow sections (SHS) beams and two rectangular hollow sections (RHS) beams were tested (Table 3.3) and moment vs. rotation curves were presented (Figure 3.2). The rotation was obtained from deflection measurements at the mid-span and at

distances of 50 mm from the supports. The experimental work was accompanied by a numerical study using the general purpose finite element software package ABAQUS. Based on additional parametric finite element analyses, the authors concluded that current European slenderness limits associated with the definitions of slender and non-slender elements need to be relaxed. It was also concluded that current American and Australian/New Zealand design rules are more reasonable than those of the Eurocode when predicting the flexural strength of lean duplex stainless steel grades.

Table 3.3. Dimension of S32012 beams used for three-point flexure test from Theofanous and Gardner (2010)

Tested Beam	Total Length (in)	Span length (in)	d (in)	b (in)	t (in)	Cross-section Shape
SHS 100x100x4-B1	51.18	43.31	4.03	4.06	0.154	
SHS 100x100x4-B2	51.18	43.31	4.04	4.02	0.151	
SHS 80x80x4-B1	51.18	43.31	3.13	3.15	0.148	
SHS 80x80x4-B2	51.18	43.31	3.13	3.15	0.147	
SHS 60x60x3-B1	51.18	43.31	2.36	2.36	0.124	
SHS 60x60x3-B2	51.18	43.31	2.36	2.36	0.122	
*RHS 80x40x4-B1	51.18	43.31	3.15	1.54	0.149	
*RHS 80x40x4-B2	51.18	43.31	3.15	1.56	0.151	

\* The RHS beams were tested about their major axis of bending (x-axis)

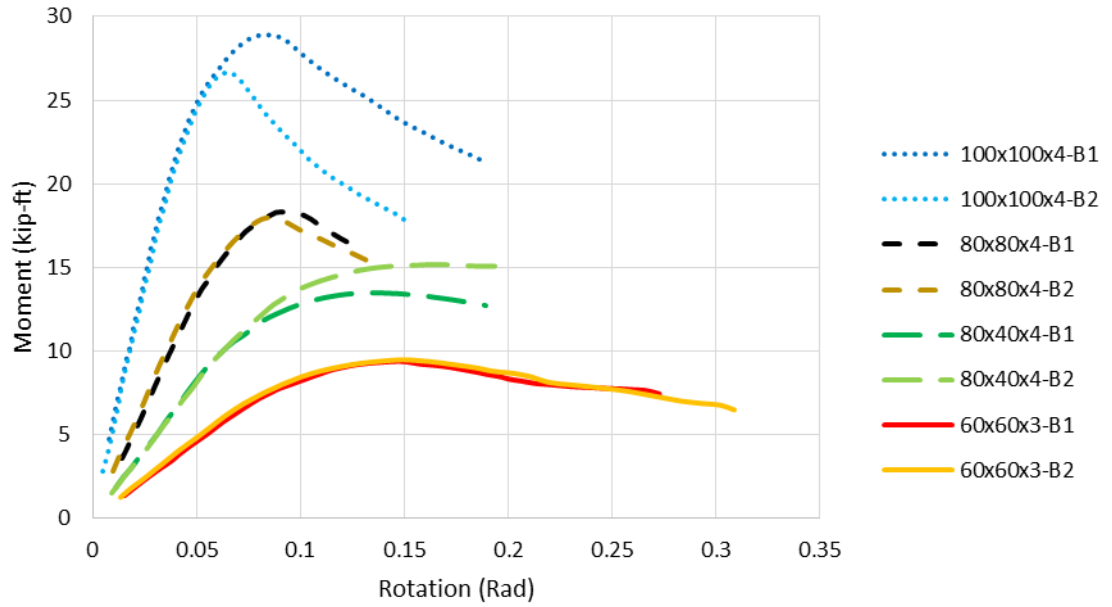
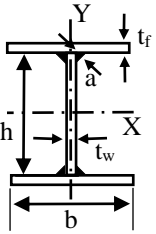


Figure 3.2. Moment vs rotation curves for SHS and RHS S32101 beams from Theofanous and Gardner (2010)

**Saliba and Gardner (2012):** In this work, eight welded S32101 lean duplex stainless steel (LDSS) I-sections were tested in flexure. The dimensions of the four I-sections subjected to a three-point bending test are shown in Table 3.4. The authors did not present directly the load-deflection curves but provided moment rotation curves for tests conducted under 3-point and 4-point loading configuration. Figure 3.3 shows the moment rotation curves for the beams subjected to 3-point bending tests. The conclusion of this study was similar to that of Theofanous and Gardner (2010), in which modification to section classification limits of Part 1.4 of Eurocode 3 was proposed.

Table 3.4. Dimensions of S32101 beams used for three-point flexure test from Saliba and Gardner (2012)

Tested Beam	Total Length (in)	Span length (in)	h (in)	b (in)	t <sub>f</sub> (in)	t <sub>w</sub> (in)	a (in)	Cross-section Shape
I-200x140x6x6	118.11	110.24	7.95	5.47	0.24	0.24	0.2	
I-200x140x8x6	118.11	110.24	7.88	5.47	0.32	0.24	0.2	
I-200x140x10x8	118.11	110.24	7.82	5.47	0.40	0.31	0.24	
I-200x140x12x8	118.11	110.24	7.83	5.48	0.49	0.32	0.24	

\* a is the weld throat

\* The I-sections were tested about their major axis of bending (x-axis)

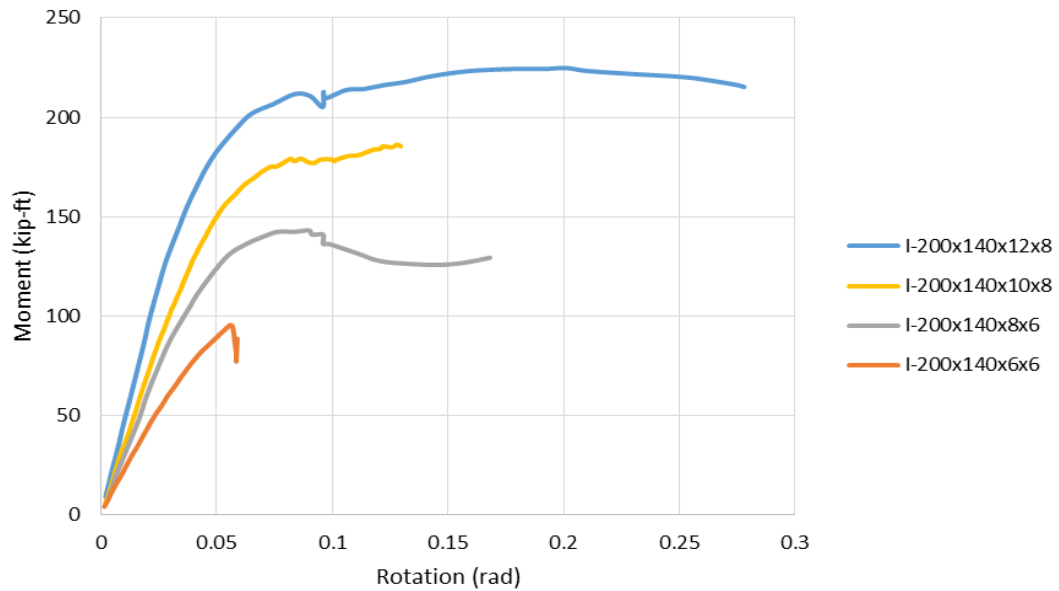


Figure 3.3. Moment vs. rotation curves from 3-point bending test for four I-section S32101 beams from Saliba and Gardner (2012)

In all of the above studies, it was evident that the deflection behavior of stainless steel beams subjected to transverse loads exhibits a non-linear trend that must be examined further in order not only to address deflection design criterion but also to develop standardized test methods at the coupon level.

## **CHAPTER 4**

### **EXPERIMENTS**

Presented in this work are the results of twelve flexural tests conducted on small-scale coupons to establish the load-deflection behavior of UNS S32003 (ATI 2003®) hot-rolled duplex stainless steel flat plates. All specimens were tested as simply supported beams loaded at the midspan. Test specimens had nominal width and thickness of 1 in. and 0.25 in., respectively. Four different span lengths of 4 in., 6 in., 9 in., and 12 in. were investigated. Analyses of the results showed that the non-linear deflection behavior can be estimated reasonably well by adopting the conventional deflection equation pertaining to an assumed linear elastic material, but after replacing the modulus of elasticity with a secant modulus corresponding to the maximum tension strain resulting from the applied load.

#### **4.1 Test Specimen Material**

The material selected for this study is UNS S32003 (ATI 2003®) hot-rolled duplex stainless steel. This grade of stainless steel offers many advantages when considering mechanical and corrosion properties, weldability, and cost. UNS S32003 stainless steel has a critical pitting temperature (CPT) and a critical crevice temperature (CCT) values of about 35°C and 16°C, respectively (Allegheny Technologies Inc. 2010). The S32003 stainless steel's calculated pitting resistance equivalent number (PREN), using equation 2.1, is in the range of 29 to 35. These indicators are shown graphically with respect to other grades of stainless steel in Figures 4.1 and 4.2. S32003 stainless

steel can also be welded using common welding procedures such as the gas metal arc welding (GMAW), the gas tungsten arc welding (GTAW), and the submerged arc welding (SAW) methods along with AWS ER2209 filler metal (Allegheny Technologies Inc. 2010). To achieve desirable impact strength and corrosion resistance, the weld and the heat-affected zone (HAZ) should have a sufficient amount of austenite. This can be accomplished by limiting the heat exposure time to the range of 650 to 1000°C (1200 to 1830°F) in order to minimize precipitation of deleterious phases that may affect both corrosion resistance or mechanical properties of the S32003 stainless steel. Typical Charpy impact energy values associated with the base metal, the weld, and the heat affected zones for the S32003 stainless steel at various temperatures below the room temperature are shown in Figure 4.3. Nominal values of the yield stress, tensile stress, and elongation for welded and non-welded S32003 stainless steel are shown in Table 4.1.

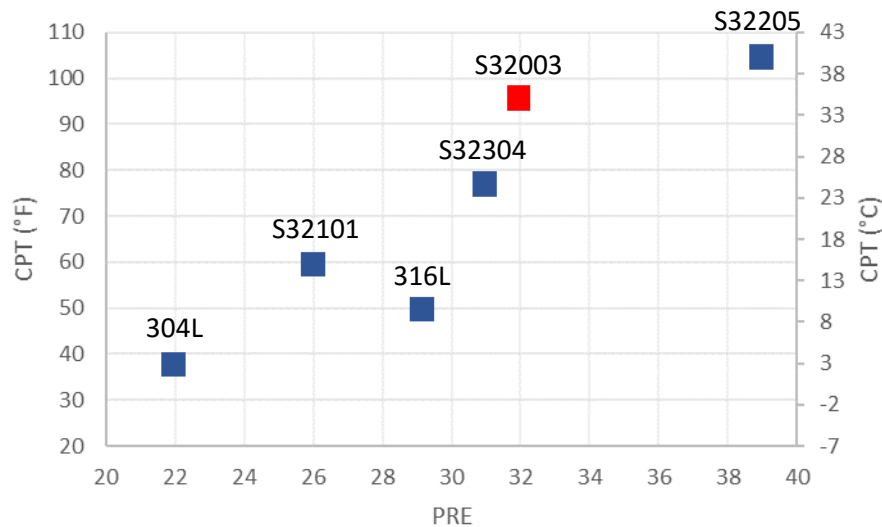


Figure 4.1. Critical Pitting Temperature (CPT) of austenitic and duplex stainless steels

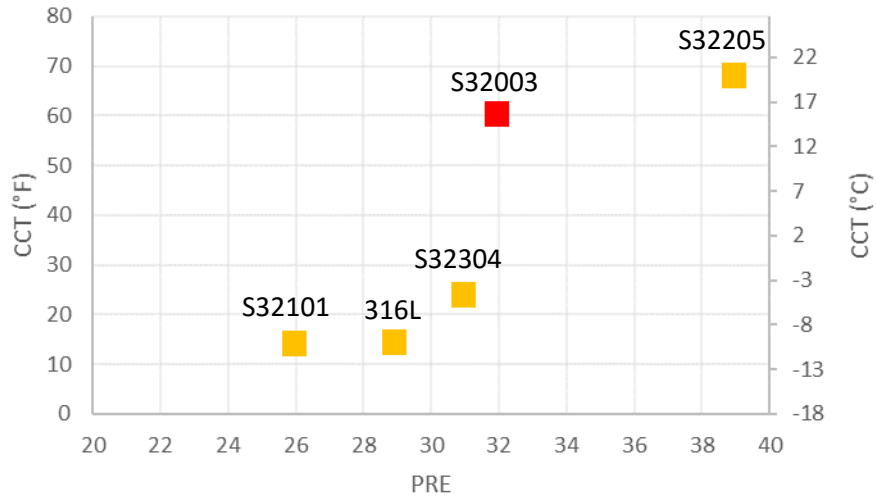


Figure 4.2. Critical Crevice Temperature (CCT) of austenitic and duplex stainless steels

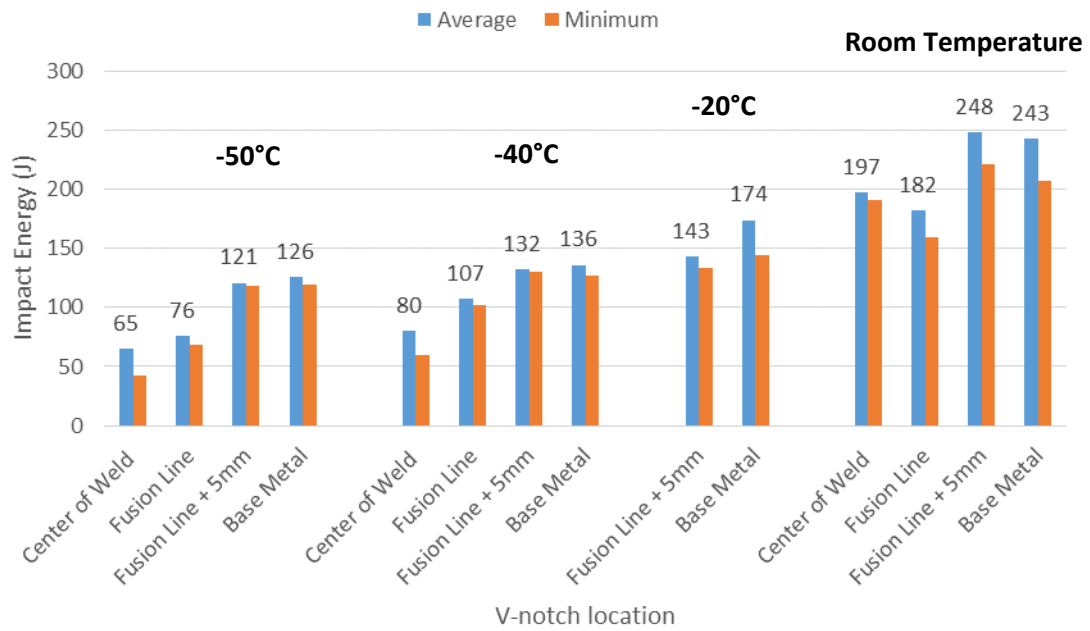


Figure 4.3. Results of charpy impact test on S32003 welded plate (ATI Allegheny Ludlum 2010)

Table 4.1. Results from tensile testing on welded S32003 samples

Properties	Welded	Non-Welded
<b>Yield Strength (0.2% offset)</b>	78 ksi (538 MPa)	77.5 ksi (534 MPa)
<b>Tensile Strength</b>	107 ksi (738 MPa)	108 ksi (745 MPa)
<b>Elongation</b>	39%	40%
<b>Break Location</b>	Base Metal	Base Metal

## 4.2 Tests Specimens

For a simply supported beam, of a span  $L$ , subjected to a concentrated load,  $P$ , at mid-span, the deflection,  $\delta$ , under the point load can be computed from the following equation:

$$\delta = \frac{PL^3}{48EI} + \frac{PL}{4\alpha GA} \quad (4.1)$$

Where the first and second terms represent the deflection due to flexure and shear, respectively. In these terms

$E$  = flexural modulus of the material

$I$  = moment of inertia of the cross-section about the axis of bending

$G$  = shear modulus of the material

$A$  = area of the beam cross-section

$\alpha$  = shear coefficient dependent on the shape of the beam cross-section

As the beam becomes shorter and shorter, the deflection due to shear deformation becomes more pronounced. This can be illustrated by computing the following ratio of the deflection due to shear to that due to flexure:

$$e = \frac{\frac{PL}{4\alpha GA}}{\frac{PL^3}{48EI}} = \frac{12}{\alpha} \frac{E}{G} \frac{I}{A} \frac{1}{L^2} \quad (4.2)$$

For a beam with a rectangular cross section of width  $b$  and thickness  $t$ ,  $A = bt$  and  $I = bt^3/12$ . Thus, Eq. 4.2 can be written in the form:

$$e = \frac{\frac{PL}{4\alpha GA}}{\frac{PL^3}{48EI}} = \frac{E}{\alpha G} \frac{t^2}{L^2} \quad (4.3)$$

For a beam with a rectangular cross section, the shear coefficient  $\alpha$  was shown by Cowper (1966) to take the following form:

$$\alpha = \frac{10(1+\nu)}{12+11\nu} \quad (4.4)$$

Results of tests reported by Reynolds (2013) and by Zureick et al. (2013) indicated that Poisson's ratio for the S32003 duplex stainless steel ranges from approximately 0.2 to 0.3. This results in a shear coefficient in the range of 0.84 to 0.85. Using a value  $E/G$  of approximately 2.8 and a value of  $\alpha = 0.84$ , Eq. 4.3 can be arranged in the form:

$$\frac{L}{t} = \frac{1.826}{\sqrt{e}} \quad (4.5)$$

When the shear deflection contribution is limited to 2% or less of that due to bending ( $e = 0.02$ ), the span to thickness ratio of the test specimen must be  $L/t \geq 12.9$ . For a material thickness of  $t = 0.25$  in., the test span shall be greater than 3.23 in. On this basis, four test spans equal to 4 in., 6 in., 9 in., and 12 in. were selected. Presented in Table 4.2, are the measured dimensions of all test specimens.

Table 4.2. Test Specimen dimensions

<b>ID</b>	<b>Total Length (in.)</b>	<b>Span, L (in.)</b>	<b>Width, b (in.)</b>	<b>Thickness, t (in.)</b>	<b>L/t</b>	<b>Area, A (in.<sup>2</sup>)</b>
<b>SSF4-1</b>	8	4	1.060	0.249	16.1	0.264
<b>SSF4-2</b>	8	4	1.021	0.248	16.2	0.253
<b>SSF4-3</b>	8	4	0.981	0.248	16.1	0.243
<b>SSF6-1</b>	8	6	1.055	0.252	23.9	0.265
<b>SSF6-2</b>	8	6	0.964	0.250	24.0	0.241
<b>SSF6-3</b>	8	6	1.016	0.250	24.0	0.254
<b>SSF9-1</b>	14	9	0.956	0.248	36.4	0.237
<b>SSF9-2</b>	14	9	1.041	0.248	36.3	0.258
<b>SSF9-3</b>	14	9	1.007	0.248	36.3	0.250
<b>SSF12-1</b>	14	12	1.024	0.248	48.4	0.254
<b>SSF12-2</b>	14	12	1.047	0.248	48.5	0.259
<b>SSF12-3</b>	14	12	1.031	0.247	48.5	0.255

### 4.3 Testing Procedure and Results

All specimens were tested in INSTRON universal testing machine with a flexural test fixture having continuously adjustable spans. The test setup is shown in Figure 4.4. After positioning the test specimen in the test fixture, a preload of about 20 lbs was applied at midspan. Once the span length and the load position at midspan were verified, the load was increased monotonically at the rate of 0.0079 in/sec. Load and displacement were recorded continuously. When the specimen displacement was increased without any

significant increase in the load, the test was terminated. The load-deflection curves of all test specimens are shown in Figures 4.5, 4.6, 4.7, 4.8, and 4.9.

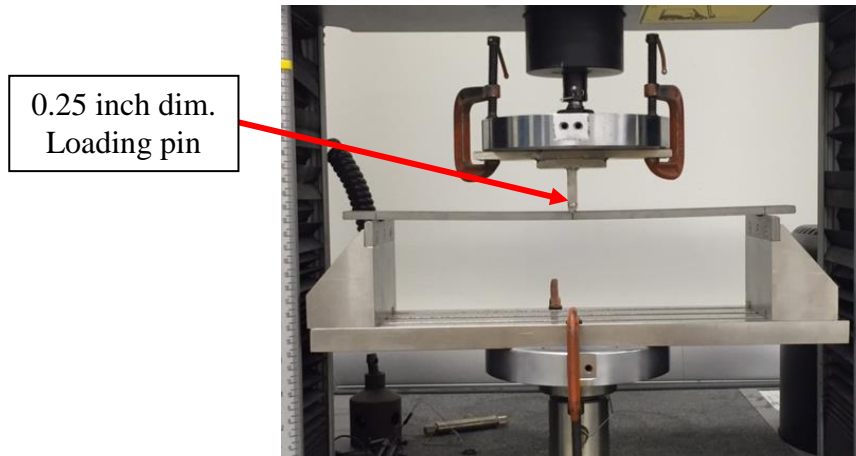


Figure 4.4. Three-point flexural test set up

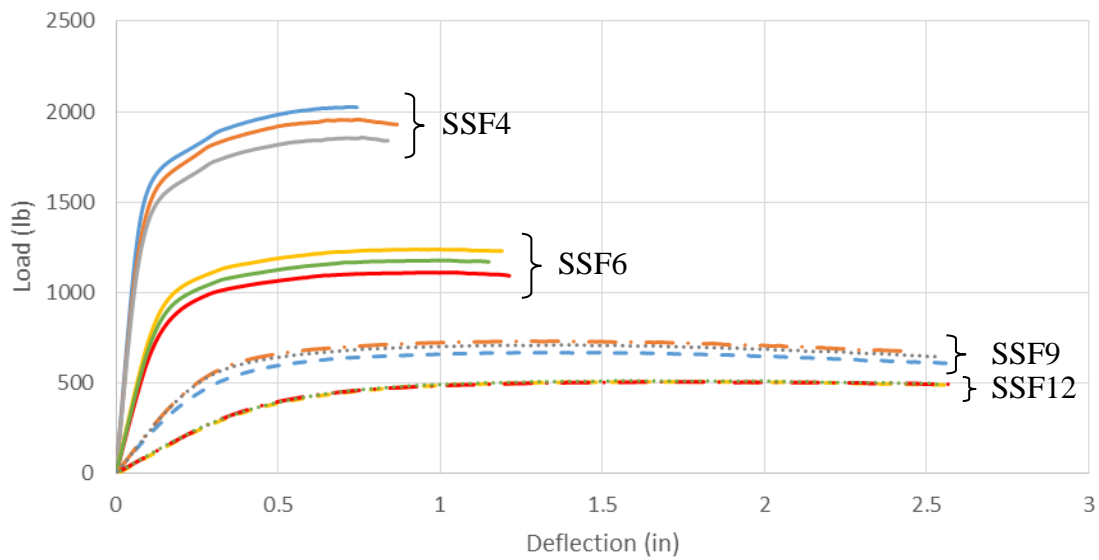


Figure 4.5. Load-deflection curves of all specimens

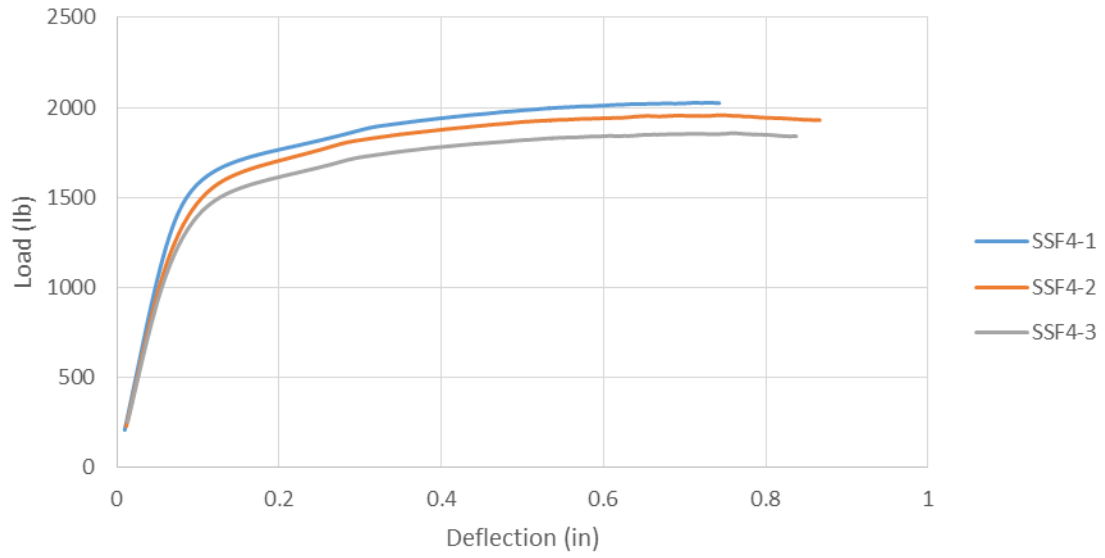


Figure 4.6. Load-deflection curves of specimens with 4in span length

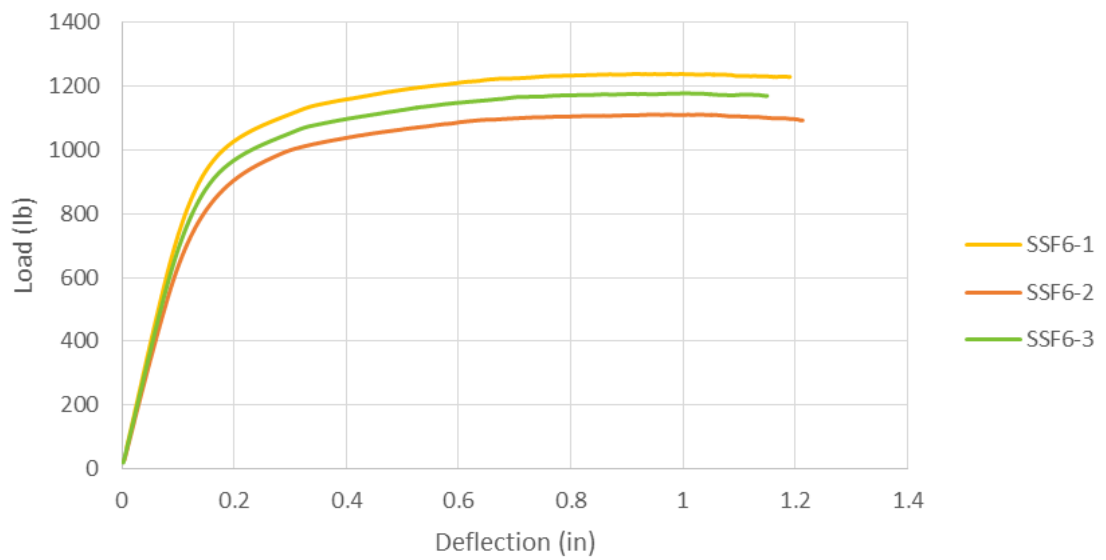


Figure 4.7. Load-deflection curves of specimens with 6in span length

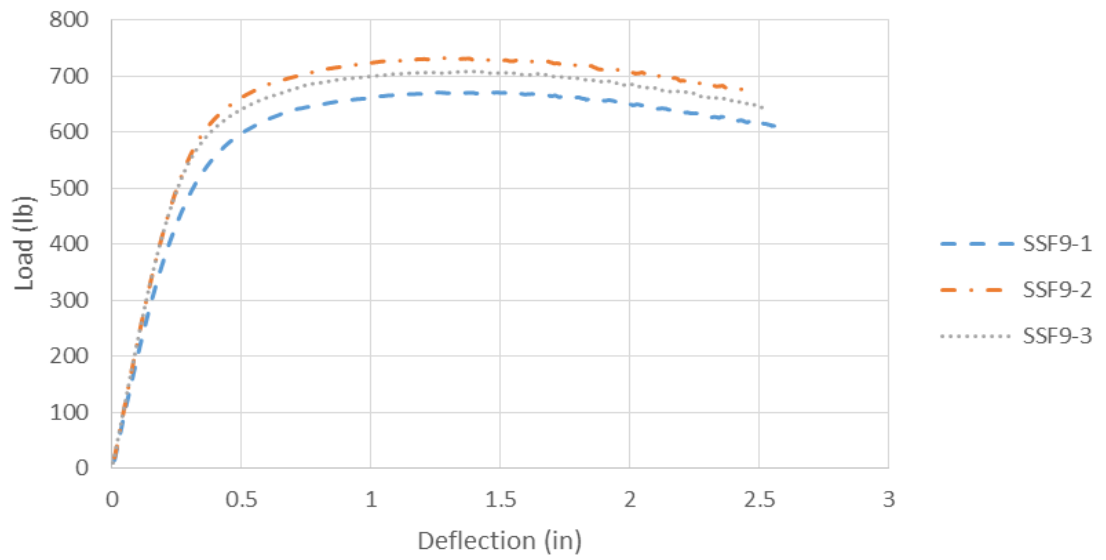


Figure 4.8. Load-deflection curves of specimens with 9in span length

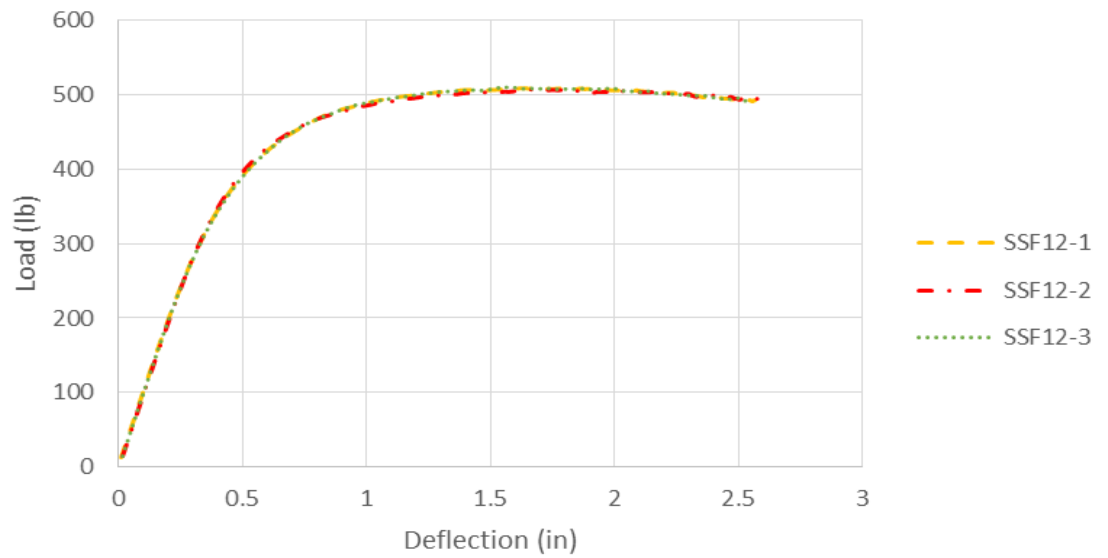


Figure 4.9. Load-deflection curves of specimens with 12in span length

#### 4.4 Analyses of Results

Since all test specimens have a span-to-thickness ratio greater than 12.9, it can be reasonably assumed that the deflection due to shear deformation is negligible. Therefore, the mid-span deflection of a simply supported beam subjected to a concentrated load at mid-span is given as follows:

$$\delta = \frac{PL^3}{48EI} \quad (4.6)$$

Due to the nonlinearity of the stress-strain curves of all tested specimens, a single value of the modulus of elasticity will not be appropriate for use in Eq. 4.6 for predicting the deflection of the test specimens. Johnson and Winter (1966) suggested that the deflection calculation of stainless steel flexural members be performed using an average secant modulus that can be expressed in the form:

$$E_{as} = \frac{E_{ts} + E_{cs}}{2} \quad (4.7)$$

$E_{ts}$  and  $E_{cs}$  are the tensile and compression secant moduli corresponding to the values of the maximum tension and maximum compression stresses in the extreme fibers of the beam, respectively. As a simplified engineering approximation for calculating the deflection of S32003 stainless steel material, attempt in this work is made to adopt a single modulus equal to the secant modulus of elasticity in tension and assume that the moduli in tension and compression are equivalent. For doing so, the tension stress-strain relationship for S32003 stainless steel is represented by the Ramberg-Osgood equation expressed in the form:

$$\varepsilon = \frac{\sigma}{E_0} + 0.002 \left( \frac{\sigma}{\sigma_y} \right)^n \quad (4.8)$$

For which the secant modulus can be derived in the form:

$$E_s = \frac{\sigma}{\varepsilon} = \frac{E_0}{1 + 0.002 E_0 \left( \frac{\sigma^{n-1}}{\sigma_y^n} \right)} \quad (4.9)$$

Where  $E_0$  is the initial modulus,  $\sigma_y$  is the yield stress, and  $n$  is a material constant. From the work of Zureick et al. (2013) who conducted tension tests on S32003 stainless steel, average values of  $E_0$  and  $\sigma_y$ , and  $n$  can be taken as 26,000 ksi, 85 ksi, and 5, respectively. By doing so, Eq. 4.8 and 4.9 become

$$\varepsilon = \frac{\sigma}{26,000} + 0.002 \left( \frac{\sigma}{85} \right)^5 \quad (4.10)$$

$$E_s = \frac{\sigma}{\varepsilon} = \frac{E_0}{1 + \frac{52}{(85)^5} \sigma^{n-1}} \quad (4.11)$$

## 4.5 Deflection Calculation Method

Deflection calculations of S32003 stainless steel flexural specimens tested at various span lengths were accomplished by adopting the following steps:

**Step 1:** Establish the mathematical model describing the tensile stress-strain behavior for S32003 stainless steel material up to the yielding stress, using Eq. 4.10.

**Step 2:** Establish the cross-section strain and stress distributions for a flexural specimen at a maximum strain of  $\epsilon_{\max}$  as shown in Figure 4.10. A stress value corresponding to a specific strain value can be computed from Eq. 4.10.

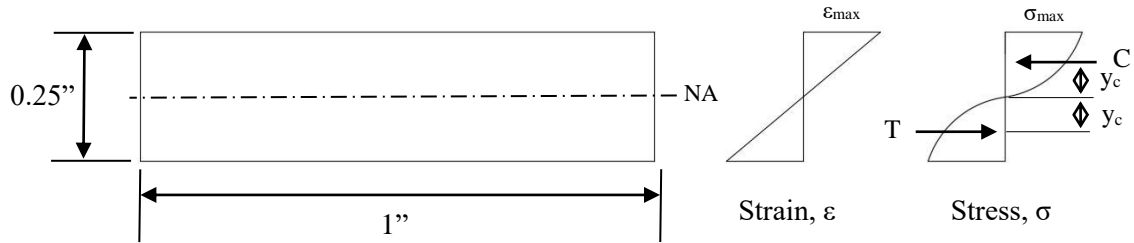


Figure 4.10. Cross-section strain and stress distribution of S32003 duplex stainless steel

**Step 3:** Calculate the compression and the tension forces resulting from the stress distribution over the cross section

$$C = T = \int_0^{t/2} b\sigma(y)dy \quad (4.12)$$

**Step 4:** Calculate the location of the compression/tension force with respect to the neutral axis, using the following equation:

$$y_c = \frac{\int_0^{t/2} y\sigma(y)dy}{\int_0^{t/2} \sigma(y)dy} \quad (4.13)$$

**Step 5:** Calculate the resulting moment and applied load as follows

$$M = C (2y_c) \quad (4.14)$$

$$P = \frac{4M}{L} \quad (4.15)$$

**Step 6:** Calculate the secant modulus (Johnson and Winter 1966) corresponding to the values of the maximum tension/compression stress in the extreme fibers of the beam using the following equation:

$$E_s = \frac{\sigma}{\varepsilon_{\max}} = \frac{E_0}{1 + 0.002E_0 \left( \frac{\sigma_{\max}^{n-1}}{\sigma_y^n} \right)} \quad (4.16)$$

When the above procedure was implemented, the computed deflection values, up to the yield stress of the material, were closely related to the experimental deflection values of all test specimens. The computed deflection values of all specimens are plotted side-by-side with the experimental results as shown in Figures 4.11, 4.12, 4.13, and 4.14. The computed deflection curves are terminated beyond the yield stress.

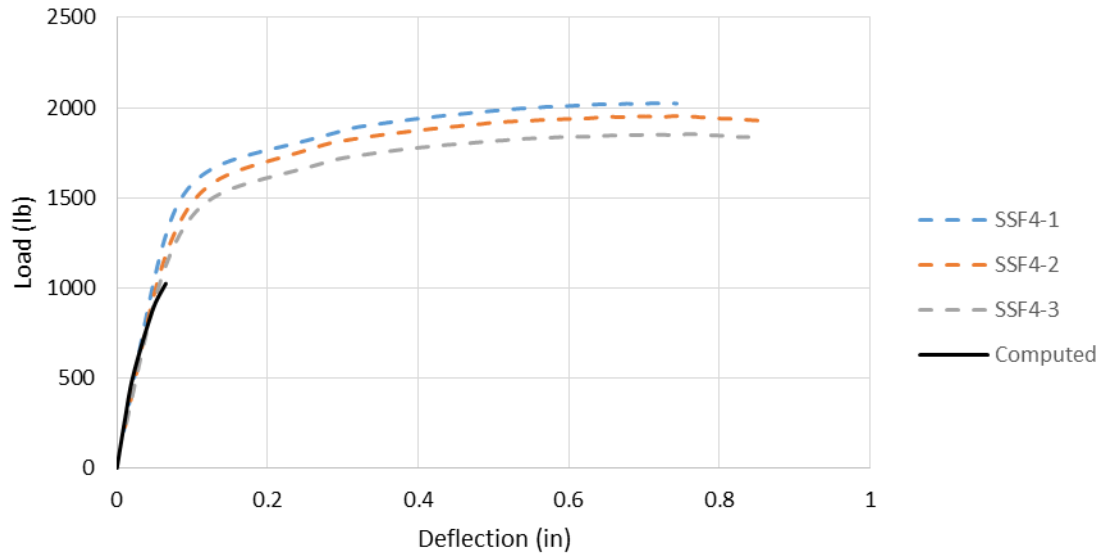


Figure 4.11. Experimental and theoretical results of load-deflection curves for specimens with 4in span length

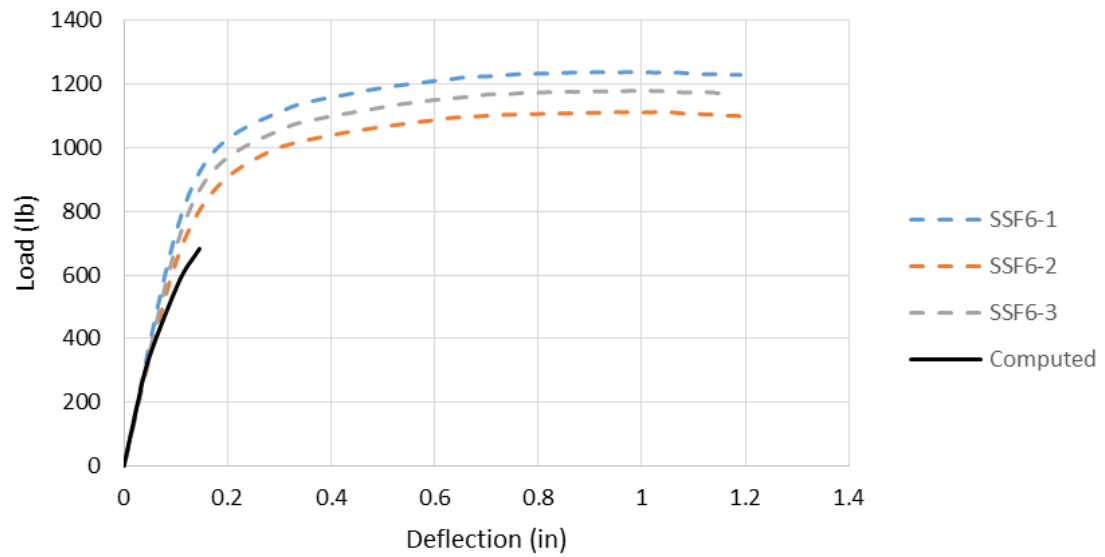


Figure 4.12. Experimental and theoretical results of load-deflection curves for specimens with 6in span length

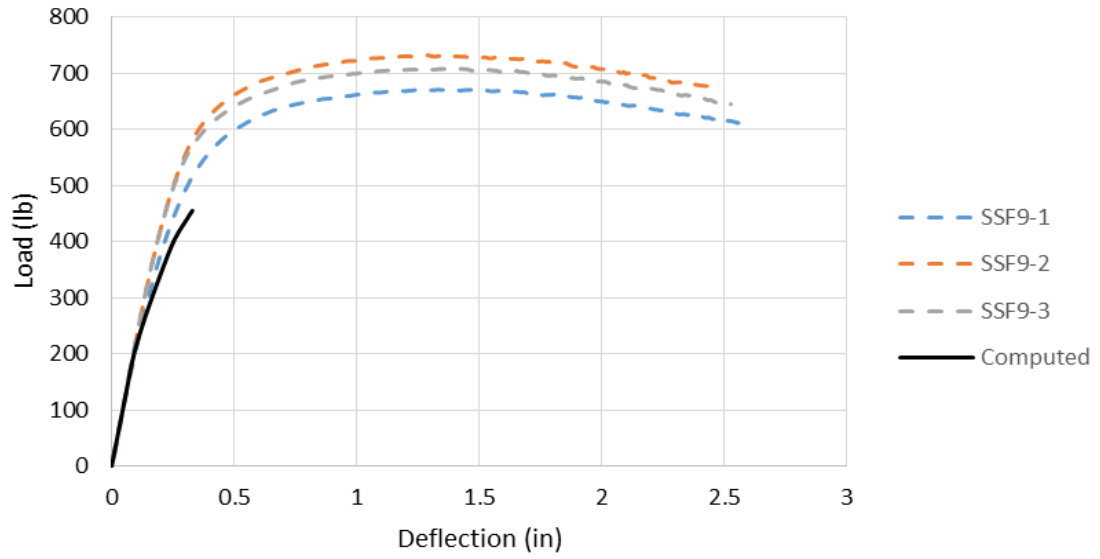


Figure 4.13. Experimental and theoretical results of load-deflection curves for specimens with 9in span length

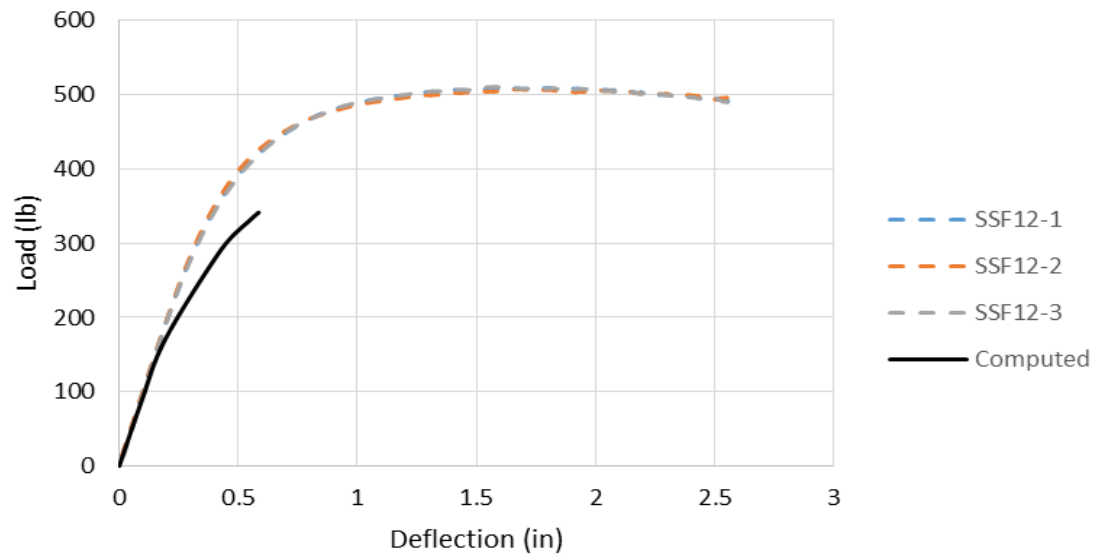


Figure 4.14. Experimental and theoretical results of load-deflection curves for specimens with 12in span length

## **CHAPTER 5**

### **CONCLUSIONS AND RECOMMENDATIONS**

Based on the work performed in this research, it is concluded that the deflection of S32003 stainless steel coupons subjected to transverse loads can be reasonably estimated by

- 1) Assuming that the tensile and compressive stress-strain curves are identical.
- 2) Using the classical small beam deflection formula for linearly elastic material but after replacing the flexural modulus with a secant flexural modulus corresponding to the values of the maximum tension or compression stress at the extreme fibers of the cross section.

The above calculation method is based on testing conducted on coupons having a small thickness of 0.25 in. For this reason, it is recommended that the validity of the deflection calculation approach reached in this study be examined on full-scale beams having a variety of cross sections and sizes.

The deflection calculation above was also limited to a state of strain below the yield strain of the material. Thus, it is recommended that this method of calculation be extended for cases in which the maximum strain in the flexural member exceeds the material yield strain.

## REFERENCES

- AISI (1988). "Welding of Stainless Steels and Other Joining Methods," *A Designers' Handbook Series*, N 9002, American Iron and Steel Institute, Washington, DC.
- ASTM (2009), *Standard Terminology Relating to Methods of Mechanical Testing*, ASTM E6-09be1, American Society for Testing and Materials, West Conshohocken, PA.
- ASTM (2010), *Standard Test Method for Young's Modulus, Tangent Modulus, and Chord Modulus*, ASTM E111-04 (2010), American Society for Testing and Materials, West Conshohocken, PA.
- ASTM (2011), *Standard Test Methods for Pitting and Crevice Corrosion Resistance of Stainless Steels and Related Alloys by Use of Ferric Chloride Solution*, ASTM G48-11, American Society for Testing and Materials, West Conshohocken, PA.
- ASTM (2012), *Standard Terminology and Acronyms Relating to Corrosion*, NACE/ASTM G193-12d, American Society for Testing and Materials, West Conshohocken, PA.
- ASTM (2013), *Standard Test Method for Linear-Elastic Plane-Strain Fracture Toughness  $K_{Ic}$  of Metallic Materials*, ASTM E399-12e3, American Society for Testing and Materials, West Conshohocken, PA.
- ASTM (2015a), *Standard Test Method for Detecting Detrimental Phases in Lean Duplex Austenitic/Ferritic Stainless Steels*, ASTM A1084-15a, American Society for Testing and Materials, West Conshohocken, PA.
- ASTM (2015b), *Standard Specification for Chromium and Chromium-Nickel Stainless Steel Plate, Sheet, and Strip for Pressure Vessels and General Applications*, ASTM A240/A240M-15a, American Society for Testing and Materials, West Conshohocken, PA.
- ATI Allegheny Ludlum (2010). "ATI 2003 Technical Data Sheet." A. Properties, ed
- ATI Allegheny Ludlum (2010). "ATI 2003 Weld Procedure and Evaluation." A. Properties, ed.

AWS (2007), *Structural Welding Code-Stainless Steel*, AWS D1.6/D1.6M:2007, American Welding Society, Miami, FL.

CW staff. (2013). “Doha’s Hamad International Airport to open April 1” <  
<http://www.constructionweekonline.com/article-20545-dohas-hamad-international-airport-to-open-april-1/>> (Sept. 20, 2015).

Gunn, R. N. (1997). *Duplex Stainless Steel*, Cambridge, England.

International Molybdenum Association (IMOA), (2014). *Practical Guidelines for the Fabrication of Duplex Stainless Steel*, 3<sup>rd</sup> Ed. London, UK.

Lula, R. A. (1986). *Stainless Steel*, Metals Park, Ohio.

Parr, G. J., and Hanson, A. (1966). *An Introduction to Stainless Steel*, Natrona Heights, PA.

Rasmussen, K. J. (2003), “Full-range stress–strain curves for stainless steel alloys”, *Journal of Constructional Steel Research*, 59, 47-61.

Rasmussen, K., and Hancock, G (1993), 'Design of cold-formed stainless steel tubular members; beams', *Journal of Structural Engineering*, 119, 2368-2386.

Reynolds, R. A., (2013). "Behavior and Design of Concentrically Loaded Duplex Stainless Steel Single Equal-Leg Angle Struts," thesis, presented to Georgia Institute of Technology, GA, in partial fulfillment of the requirements for the degree of Doctor of Philosophy.

Saliba, N., and Gardner, L. (2013). “Cross-section stability of lean duplex stainless steel welded I-sections”, *Journal of Constructional Steel Research*, 80, 1-14.

SCI (2006). “Design manual for structural stainless steel, 3<sup>rd</sup> Edition”, The Steel Construction Institute, United Kingdom.

Tavares, S., Pardal, J., De Abreu, H., Dos Santos Nunes, C., and Da Silva, M. (2012). “Tensile properties of duplex UNS S32205 and lean duplex UNS S32304 steels and the influence of short duration 475 °C aging,” *Materials Research*, 15, 6, 859-864.

Theofanous, M., and Gardner, L (2010). “Experimental and numerical studies of lean duplex stainless steel beams,” *Journal of Constructional Steel Research*, 66, 816-825.

Withnell, R. (2015). “Cruising to Holyhead”  
<<http://www.bikesandtravels.com/biker.aspx?ride=780>> (Sept. 20, 2015).

Wright, W., J. (2012). *Steel Bridge Design Handbook: Bridge Steels and Their Mechanical Properties*. Vol. 1, Washington, DC.

Zureick, A., Ellinwood, B., Bechtel, A., Kim, S., Krapf, C., O’Malley, C., and Shah, F. (2013). “Bridge Repair and Strengthening Study Part 1”, Georgia DOT Research Project 0805.